Supplemental Materials and Methods:

Cell lines and culture. ABC-DLBCL cell lines (TMD8, OCI-Ly10, SUDHL2, and OCI-Ly3), mantle cell lymphoma cell lines (JeKo-1, Granta-519, Rec-1, Z-138 and Mino) were engineered to express the bacterial tetracycline repressor as described previously [1]. All cultures were routinely tested for Mycoplasma contamination. All lymphoma cell lines were purchased from the ATCC and used for previous studies (31, 32) and authenticated by STR profiling. Ibrutinib-resistant TMD8, OCI-Ly10, Rec-1, and JeKo-1 cells were generated by *in vitro* culture of their parental cell lines for prolonged periods of time with progressively increasing the concentrations of ibrutinib. Cell lines and their drug-resistant clones grew in RPMI-1640 medium (Life Technologies) with 10% FBS (ThermoFisher), 1mmol/L sodium pyruvate (Cytiva HyClone), and 1% penicillin/streptomycin (Life Technologies).

Measurement of mitochondrial membrane potential (ΔΨ) and mitochondrial ROS. Cells were incubated with JC-1 (10 μg/mL) for 10 min or mitoSOX (5 μM) for 20 min in phenol red free media at 37°C, followed by three washes with PBS. Subsequently samples were analyzed using an Attune flow cytometer.

Primary MCL samples

All four primary cells were gifts from Dr. Vu N. Ngo's laboratory in Beckman Research Institute of City of Hope. Primary cells were cultured in RPMI-1640 medium (Life Technologies) with 10% FBS (ThermoFisher), 1mmol/L sodium pyruvate (Cytiva HyClone), and 1% penicillin/streptomycin (Life Technologies).

Doxycycline-inducible system and retroviral transduction

Doxycycline-inducible cells lines can express the bacterial tetracycline repressor, engineered as described previously [2]. Doxycycline (20 ng/ml) was used for inducing the expression of genes of interest. 293T cells were transfected with a mixture of DNA/shRNA constructs, the mutant ecotropic envelop-expressing plasmid pHIT/EA6 × 3*, and gag-pol-expressing plasmid using PEI Transfection Reagents. The retroviral supernatants were harvested for infecting doxycycline-inducible lymphoma cells with 8 μg/ml polybrene by centrifugation at 2,500 r.p.m. for 1.5 hours. The infected cells were selected with puromycin (1 μg/ml) for 6 days, and GFP positive cells were analyzed with flow cytometry. shCtrl group refers to cells expressing a control shRNA[2,3].

Dual-luminescence-based reporter gene assay

The Dual-luminescence-based reporter gene assay was performed in triplicate at room temperature. HEK293T cells were co-transfected with CMX-β-gala (15 ng), pGL3 basic (100 ng), pGL3-PDP1 promoter region constructs ((pGL3-F1 (100 ng), pGL3-F2 (100 ng), pGL3-F3 (100 ng)) or pGL3-EGR1 promoter region constructs ((pGL3-F1 (100 ng), pGL3-F2 (100 ng), pGL3-F3 (100 ng), pGL3-F4 (100 ng)), and 200 ng PBMN vector or retro CMV vector, PBMN-OE-EGR1 or retro CMV-TCF4, respectively, using PEI. CMX-β-galactosidase expression vector (15 ng) was transfected for normalization of transfection efficiency. After 48 h, cells were harvested and lysed in lysis buffer (0.1 M potassium phosphate, pH 7.8, 0.2% Triton X-100, 0.5 mM DTT and 1 mg/mL bovine serum (BSA) Fraction V (A-3059; Sigma Chemical). Luminescence signal intensity was measured followed by Chemiluminescent Reporter Gene Assay System and Luciferase Assay System, respectively. Firefly luciferase activity from the pGL3 basic reporter was normalized with β-galactosidase activity.

XF cell mito stress analysis

The mitochondrial respiratory capacity was determined using XF Cell Mito Stress Test Kit (Agilent Technologies). 2-5 x10^5 cells per well were seeded into the Cell-Tak-Coated 96-well XF Cell Culture

Microplate and a round bottom 96 well plate. To normalize OCR per viable cell, cells in a round-bottom 96 well plate were counted using DAPI on a flow cytometer. Cells in an XF Cell Culture Microplate were incubated in analysis media separately containing 10mM glucose, or 2 mM sodium pyruvate or 2.5 mM L-glutamine. The cells were incubated in a CO2-free incubator at 37°C for 1 hour prior to assay.

The oxygen consumption rate (OCR) was measured by XF^{e}96 extracellular flux analyzer (Agilent Technologies) with sequential injection of oligomycin A (1 μM), FCCP (1 μM), and rotenone/antimycin A (0.5 μM). ATP production was calculated following the manufacturer's guidelines as: ATP = (Last rate before Oligomycin injection) - (Minimum rate after Oligomycin injection).

Pyruvate dehydrogenase enzyme activity assay

The Pyruvate dehydrogenase (PDH) Enzyme Activity Microplate Assay Kit (Abcom, ab109902) was used to measure the PDH activity, following the manufacturer's instructions. Briefly, indicated PBS with 1/9 volume detergent was added into each 1.5 ml tube with cells collected from a 10 cm dish. The tubes were kept on ice for 10 min after gentle mixing. Tubes were centrifuged at 1,000g for 10 min and the supernatant was transferred into a new tube. Protein concentration was measured with BCA and 200 μl protein lysis (0.5 – 5mg/ml) per well was loaded into a 96-well assay plate and kept at room temperature for 3 hours. Assay buffer was mixed with 100 × coupler, 100 × dye, 20 × reagent mix and 20 × sample buffer. Liquid in the assay plate wells was removed and washed twice with 1 × stabilizer. 200 μl assay buffer was added into each well, and absorbance was measured at 450 nm every 30 s for 30 cycles with a microplate reader. The slope of the kinetic cure was calculated to indicate PDH activity.

Confocal imaging

The TMD8 and OCl-Ly10 cells were fixed with 4% paraformaldehyde in culture media for 15 min at 37°C and permeabilized with 0.2% Triton X-100 for 10 min at room temperature. The nonspecific binding was blocked by incubation with 4% BSA in PBS for 60 min, and cells were subsequently stained with MitoTracker® Deep Red FM (10 nM) for 20 mins. The slides were gently washed in PBS three times (5min/each time). After being washed three time in PBS and air-dried, the coverslips were mounted in ProLong Gold anti-fade reagent with DAPI (Invitrogen). Fluorescence was examined Nikon A1RS Confocal Microscope equipped with a 60-x objective lens with laser excitation at 405nm and 638 nm**.** Images were analyzed and quantification with the ImageJ 1.5.3 software.

RNA sequencing

Total RNA was extracted using RNeasy plus mini kit (Qiagen) according to the manufacturer's protocol. RNA sequencing (RNA-seq) libraries were prepared by using the Illumina TruSeq stranded mRNA LT sample preparation kit (Illumina). Gene set enrichment analysis (GSEA) was performed by GSEA software (V2.0; http://software. broadinstitute.org/gsea/index.jsp). RNA-seq data discussed in this article have been deposited in the National Center for Biotechnology Information's Gene Expression Omnibus (GEO) and are accessible through GEO Series accession number: GSE223150.

Variant calling

Reads from RNA-sequencing were aligned to hg19 using STAR (v2.5.2b). Duplicated reads were removed with picard (v1.141). Germline SNP was called using the following tools in the Genome Analysis Toolkit (GATK v3): SPlitNCigarReads, HaplotypeCaller and VariantFiltration with default parameters except for the following:

•For HapotypeCaller, dontUseSoftChippedBases was specified, -stand_call_conf and -stand_emit_conf were both set to 20.0.

•For VariantFiltration, window was set to 35, and only variants having variant confidence greater than 2 and strand bias less than 30 were kept.

Chromatin immunoprecipitation (ChIP)
Briefly, 60 x 10^6 cells were fixed with 1% formaldehyde for 10 min at room temperature. The cross-linking reaction was stopped by addition of 1× glycine solution for 5 min. Cells were washed twice with ice-cold PBS. Cytosols were removed using ChIP cell lysis buffer. Nuclear pellets were resuspended in micrococcal nuclease buffer (MNase), treated with 112.5 unit of MNase for 12 min at 37°C and stopped by adding EDTA to the final concentration of 0.5M. Nuclear pellets were then washed once with MNase buffer, lysed with nuclear lysis buffer for 20 min at 4°C, and sonicated for a total of 5 min (5s on, 20s off, 20% amplitude, qsonica #Q500-110) at 4°C. 2% of fragmented DNA was kept as input. The remaining DNA fragments were recovered using anti-TCF4 (1 µg for 60 million cells) or anti-EGR1 (1 µg for 60 million cells), or normal rabbit anti-IgG. DNA fragments were washed and reverse crosslinked as previously described [3]. Recovered DNA fragments were purified using QIAGEN PCR purification kit and diluted in 500 1 µL of water. For each real-time PCR reaction, 3 µL was used with specific primers. The SensiFAST™ SYBR® Hi-ROX Kit (Bioline BIO-92020) was used for qPCR.

ATAC-seq regions of open chromatin peak calling, gene associations, and motif analysis
SRR42, SRR43 and SRR46 ATAC-seq data sets can be found via the SRA/NCBI BioProject (https://www.ncbi.nlm.nih.gov/Traces/study/?acc=PRJNA750745), accession PRJNA750745. TCF4 ChIP-seq data can be found via the Staudt Lab (https://lymphochip.nih.gov/local/Staudt_Ibrutinib _resistance_BCD/). Fastq files from PRJNA750745 were processed by fastp[4] and aligned to the human genome hg19 using Hisat2[5] with default parameters. Open chromatin regions were called using MACS2 [6] (parameters: -p 0.05). BedGraph files were converted into bigwig files for IGV visualization by bedGraphToBigWig function[7]. Peaks were annotated by R package ChIPseeker[8]. TxDb.Hsapiens.UCSC.hg19.knownGene and org.Hs.eg.db were used as annotation database for information such as entrez ID, ensemble, symbol, gene name and transcript ID. The sequence of peak near to gene EGR1 was extracted for transcription factor footprints analysis with ChIPpeakAnno [9]. At last, MEME-Tomtom[10,11] pipeline with default parameters was applied to search for the motifs enriched in the certain sequence. HUMAN-HOCOMOCO Human (v11 CORE) was used as motif database.

Mice. Male and female NOD.Cg-Prkdcscid Il2rgtm1Wjl/SzJ (NSG) breeder pairs were purchased from The Jackson Laboratory (Bar Harbor, ME, USA) and bred under specific pathogen-free conditions in sterile ventilated racks in the animal care facility at the University of Wisconsin-Madison and the National Cancer Institute, NIH. Both male and female mice were used between 8-16 weeks of age. The study was approved by the Animal Care and Use Committee of the University of Wisconsin-Madison (M005915) and the National Cancer Institute, NIH.

Xenograft studies
TMD8 IBR #3, OCI-Ly10 IBR#9, OCI-Ly10 IBR#10 shCtrl or OCI-Ly10 IBR#10 shEGR1 cells were inoculated subcutaneously into the flank of male and female NSG mice. When tumors reached approximately 150 mm^3, mice were randomized and administered vehicle, ibrutinib, metformin or the combination of both at the indicated doses in the figure or main text. Body weight and tumor diameter were measured twice a week, and tumor volume was determined by calculating the volume of an ellipsoid using the formula length × $width^2$ × 0.5. All values were expressed as mean ± standard error of the mean (SEM). When mice became moribund or when tumor size exceeded 20 mm in any direction, mice were euthanized as required by institutional protocols.

Drug formulation
For *in vivo* studies, ibrutinib was formulated in 5% DMSO, 30% PEG400, 5% Tween 80, and 60% water. IM156 was formulated in 2.5% DMSO, 15% PEG400, 2.5% Tweens 80, and 80% water. Metformin was formulated in 5.0 % DMSO, and 95% water. Drugs were used immediately after suspension.

Trypan blue staining
Cell viability was measured with an automatic cell counter according to the manufacturer's instruction. Cells were suspended and mixed with equal volume of 0.4% trypan blue in PBS. Ten microliters of the cell suspension were loaded onto TC20 system (Bio-Rad) counting slides, and the number of viable cells was quantified on a TC20 automated cell counter (Bio-Rad).

RT-qPCR
Total RNA was extracted using RNeasy Plus Mini Kit (Qiagen) according to the manufacturer's protocol and quantified with a Nanodrop lite spectrophotometer (Thermo Scientific). For each sample, 1.5μg RNA was reverse transcribed with a first-strand cDNA synthesis kit (Invitrogen). qPCR was performed with SensiFast SYBR Hi-Rox Kit (Bioline: BIO-92005) using an ABI Stepone Plus Real-Time PCR System. Samples were run at 2 min at 95°C, followed by 40 cycles at 95°C for 5s and 60°C for 30s. Data were normalized to β-Actin mRNA expression.

Lactate production assay
Lactate production assays are performed by following the Lactate-Glo™ Assay 's Manual (Promega). Briefly, 20,000 cells were resuspended in 25 μl PBS and plated in 96-well plates. 12.5 μl inactivate solution (0.6 N HCl) was added, mixed by shaking the plate for 5 minutes, then 12.5 μl neutralization solution was added followed by shaking 30-60 seconds. The Lactate Detection Reagent was added to 96-well plates as described in the manual and incubated 1 hour at room temperature. Then the luminescence signaling were recorded with an EnSpire plate reader (Perkin Elmer).

Western blot analysis
Cell pellets were lysed in RIPA buffer (10mM Tris-HCl, pH8 140 mM NaCl, 1mM EDTA, 0.5mM EGTA, 1% Triton X-100, 0.1% Sodium Deoxycholate, 0.1%SDS) supplemented with protease / phosphatase inhibitor for 15 mins on ice. Lysates were cleared by centrifugation at 15,000g at 4°C for 15 min and protein concentrations were determined by BCA protein assay (Pierce). 25ug of lysates were denatured with SDS sample buffer and 2.5% beta-mercaptethanol at 95°C for 5 mins. Samples were subjected to electrophoresis through a RunBlue SDS Gel 4-20% (CBS Scientific) and then immobilized on the polyvinylidene difluoride membrane (IPFL00010, Millipore). The Odyssey Imaging System (CRB LI-COR Biosciences) was used for densitometry.

IHC staining and quantification
The tumor tissues from NSG mice were fixed and embedded with paraffin after those mice were sacrificed. Immunohistochemical staining of samples were performed by the Experimental Animal Pathology Laboratory at the Carbone Cancer Center (Madison, WI). The primary antibody of rabbit anti-Ki-67 and cleaved Caspase 3 were used. Three tumor tissues were collected from each group to stain, and four images from each staining were taken. Protein expression was quantified using Image J 1.5.3 software.

REAGENT or RESOUECE	SOURCE	IDENTIFER
Antibodeis		
Rabbit monoclonal anti-EGR1 (44D5)	Cell signaling	4154S
Rabbit monoclonal anti-BTK (D3H5)	Cell signaling	8547
Rabbit monoclonal anti-PDP1 (D8Y6L)	Cell signaling	65575
Rabbit monoclonal anti-beta-Actin	Cell signaling	4967S
Rabbit polyclonal anti-Cleaved Caspase-3 (Asp175) (5A1E)	Cell signaling	9664
Rabbit monoclonal anti-human Ki-67 (D2H10)	Cell signaling	9027
Anti-rabbit IgG, HRP-linked Antibody	Cell signaling	7074
Anti-mouse IgG, HRP-linked Antibody	Cell signaling	7076
Rabbit polyclonal anti-Pyruvate Dehydrogenase E1-alpha subunit (p Ser293)	Novus Biologicals™	NB11093479T
Mouse monoclonal anti-PDH-E1α Antibody (D-6)	Santa cruz	sc-377092
Mouse monoclonal anti-EGR1(B6)	Santa Cruz	sc-515830
Mouse monoclonal antibody LDH-A(E9)	Santa Cruz	sc-137243
Mouse monoclonal anti-alpha tubulin (TU-02)	Santa cruz	sc-8035
Mouse monoclonal anti-FLAG® M2 antibody	Sigma-Aldrich	F1804
Rabbit polyclonal anti-PDK1 antibody	Proteintech	18262-1-AP
Rabbit polyclonal anti-PDP2 antibody	Thermo fisher	PA5-100680
Rabbit monoclonal anti-TCF-4 antibody [NCI-R159-6]	Abcam	ab217668
Mouse monoclonal anti-Hsp90 antibody	Abcam	ab1429
PE mouse anti-human CD19 Clone 4G7	R&D biotechne	MAB4867R
PE mouse IgG1 κ Isotype Control	BD biosciences	555749
APC mouse anti-human CD38	BD biosciences	555462
APC mouse IgG1 κ Isotype Control	BD biosciences	555751
APC mouse anti-human CD45 Clone 2D1	BD biosciences	368514
PE mouse anti-human CD2	eBioscience	12-0029-41
PE mouse anti-human CD3 antibody	BD biosciences	300308
FITC mouse anti-human CD34 Clone 4H11	eBioscience	11-0349-41
FITC mouse anti-human CD20 clone LT20	Miltenyi Biotec	130-113-373
Mouse polyclonal anti-Vinculin Polyclonal	Bethyl Laboratories	A302-534A

REAGENT or RESOUECE	SOURCE	IDENTIFER
Chemicals and Critical Commercial assays		
Ibrutinib	Selkchem	S2680
IM156	Selkchem	S9604
Metformin hydrochloride	Sigma-Aldrich	PHR1084
Phenformin hydrochloride	Sigma-Aldrich	P7045
Mithramycin A	Cayman Chemical	11434
Devimistat	Targetmol	CAS 95809-78-2
JC-1 Dye	Invitrogen™	T3168
MitoSOX™ Red Mitochondrial Superoxide Indicator	Thermo Fisher Scientific	M36008
MitoTracker™ Deep Red	Thermo Fisher Scientific	M22426
Galacto-Star™ β-Galactosidase Reporter Gene Assay System	Thermo Fisher Scientific	T1012
SuperScript™ IV First-Strand Synthesis System	Thermo Fisher Scientific	18091050
SuperSignal™ West Femto Maximum Sensitivity Substrate	Thermo Fisher Scientific	34096
Pierce™ BCA Protein Assay Kit	Thermo Fisher Scientific	23225
Trizol for RNA extraction	Thermo Fisher Scientific	15596018
Luciferase Assay System	Promega	E1500
CellTiter-Glo(R) 2.0 Assay	Promega	G9242
Lactate-GloTM Assay	Promega	J5021
Pyruvate dehydrogenase (PDH) Enzyme Activity Microplate Assay Kit	Abcom	ab109902
ChromaFlash High-Sensitivity ChIP Kit (24 reactions)	EpigenTek	P-2027-24
APC BrDu flow kit	BD pharmingen	552598
APC Annexin V	BD pharmingen	550474
PI flow dye (BD)	BD pharmingen	556463
Doxycycline hyclate	SIGMA-ALDRICH	D9891
RPMI-1640 medium (1x) -L-glutamine	hyclone	SH30096.LS
DMEM/High glucose with L-glutamine, sodium pyruvate	hyclone	SH30243.FS
FBS	Atlanta	quote #50319
Seahorse XF Cell Mito Stress Test Kit	Agilent	103015
XF RPMI Medium ph7.4	Agilent	103576
XF Calibrant, ph 7.4	Agilent	100840
Corning® Cell-Tak™ Cell and Tissue Adhesive	Corning	354240
pen/strep solution	lonza	17-602E
Corning® glutagro™	Corning	25-015-CI
MEM Non-Essential Amino Acid Solution (100X)	Lonza	13-114E
Sodium Pyruvate Solution	GE Healthcare Life Sciences	SH30239.01
Trypan Blue Solution (w/v) in PBS	corning	25-900-CI
Protease inhibitor cocktail	sigma-aldrich	P8340
PMSF Protease Inhibitor	Thermo Scientific™	36978
NuPAGE™ LDS Sample Buffer (4X)	Thermo Scientific™	NP0007
D-Luciferin, Sodium Salt	Gold Biotechnology	LUCNA
QIAquick PCR Purification kit	QIAGEN	28106
RNeasy Plus Mini Kit	QIAGEN	74136
SensiFast SYBR Hi-Rox Kit	Bioline	BIO-92005
TruSeq Stranded mRNA Library Preparation Kit Set B	illumina	RS-122-2102
TruSeq DNA LT Sample Prep Kit	Illumina	FC-121-2001
Triton X-100	EMD MILLIPORE	94101L
pierce 16% formaldehyde (w/v), methanol-free	pierce	28908
PureLink™ RNase A	Invitrogen	12091021

Experimental models ; Mouse		
NSG mice	Jackson Laboratory	005557 - NOD.Cg-Prkdcscid Il2rgtm1Wjl/SzJ

Software and Algorisms		
ImageJ 142 software	NIH	https://imagej.nih.gov/ij/index.html
GraphPad Prism 9.0	Graphpad	www.graphpad.com
FlowJo Software vX 10.0.7v2	FLOWJO, LLC	
GSEA v3.0	Broad Institute	
Igtegrative Gomomic Viewer v2.3.91(145)	Broad Institute	

Recombinant DNA		
pHIT/EA6x3	Ngo, et al. Nature 2006	DOI: 10.1038/nature04687
pHIT60	Ngo, et al. Nature 2006	DOI: 10.1038/nature04687
pRetro/CMV/TO/P-EGR1	Shuichi, et al. Mol Cancer Res 2021	DOI: 10.1158/1541-7786.MCR-21-0267
pRSMX-PG-shEGR1#8	Shuichi, et al. Mol Cancer Res 2021	DOI: 10.1158/1541-7786.MCR-21-0267
pRSMX-PG-shEGR1#9	Shuichi, et al. Mol Cancer Res 2021	DOI: 10.1158/1541-7786.MCR-21-0267
pRSMX-PG-shRNA control	Shaffer, et al. Nature 2008	DOI: 10.1038/nature07064
pLKO.5 control sh	SHC202	Sigma
pLKO.5-shTCF4 (CDS) #1	TRCN0000274162	Sigma
pLKO.5-shTCF4 (3UTR) #2	TRCN0000274213	Sigma
pGL3-F1 (94928900-94929460)	This paper	
pGL3-F2 (94928900-94929180)	This paper	
pGL3-F3 (94929181-94929460)	This paper	

Oligo Name	Sequence	Application
human EGR1 mRNA F	TGACCGCAGAGTCTTTTCCT	qRT-PCR (mRNA)
human EGR1 mRNA R	TGGGTTGGTCATGCTCACTA	qRT-PCR (mRNA)
human beta-Actin mRNA F	AAACTGGAACGGTGAAGGTG	qRT-PCR (mRNA)
human beta-Actin mRNA R	AGAGAAGTGGGGTGGCTTTT	qRT-PCR (mRNA)
human PCNA mRNA F	AGGCACTCAAGGACCTCATC	qRT-PCR (mRNA)
human PCNA mRNA R	GCCAAGGTATCCGCGTTATC	qRT-PCR (mRNA)
human 94928900-PDP1-Fragement 1-Kpn1-Forward	CGGGGTACC CCTTCCACTCGCTGGGGG	PDP1 promoter DNA

human 94929180 PDP1-Fragement 1 -Xho1-Reverse	CCGCTCGAG CACTCTGCTCCCCTACCGTG	PDP1 promoter DNA
human 94929181 PDP1-Fragment 2 -Kpn1-Forward	CGGGGTACC GGCAGGCCGGGGGTGAGG	PDP1 promoter DNA
human 94929460 PDP1-Fragment 2 -Xho1-Reverse	CCGCTCGAG CGCCCGGCGCGCACCTGG	PDP1 promoter DNA
EGR1 promoter region #1F	GGTGAAACCTGGTCTCTACTAAA	
EGR1 promoter region #1R	CCTCCTGGGTTCAAGCTATTT	
EGR1 promoter region #2F	CCTCACCACAAGGACCATTATC	
EGR1 promoter region #2R	CGAAAGGCTGTTCCCTAGTC	
EGR1 promoter region #3F	AAGGCAGCTCACTGCTATAC	
EGR1 promoter region #3R	TCTATGGCACGGTGTCTTTC	
EGR1 promoter region #6F	CAGCAACAGCAGCAGCA	
EGR1 promoter region #6R	TCCGCCTGAGGGTTGAA	
DNLZ-F	AGGAAAGCCGAGGATGACTT	
DNLZ-R	TCATGGTGAGTTGAGGGAGA	
Arid3-F	CTCAGGGTCTCTCCGTCTAA	
Arid3-R	GACCAAGTCTCTTCCCTTCTTAC	
Chr.5-F	CCTGGATATGGTCTCCCTGAT	
Chr.5-R	CCTGGCCTGACTTTGTCTTT	
EGR1 Promoter-Set1-Forward-Xho1	CCG CTCGAG GAAAGACACCGTGCCATAGA	
EGR1 Promoter-Set1-Reverse-Hind III	CCC AAGCTT TATCGGGCCACTCCAAATAAG	
EGR1 Promoter-Set2-Forward-Xho1	CCG CTCGAG CTCACCACAAGGACCATTATCT	
EGR1 Promoter-Set2-Reverse-Hind III	CCC AAGCTT TCGCTGGGAAATTGAGGATAG	
EGR1 Promoter-Set3-Forward-Xho1	CCG CTCGAG CTCCTGGTGAGAACAAGAATCA	
EGR1 Promoter-Set3-Reverse-Hind III	CCC AAGCTT AAATAAGGTGCTGCCCAAATAAG	
EGR1 Promoter-Set4-Forward-Xho1	CCG CTCGAG ATTTGGAGTGGCCCGATATG	
EGR1 Promoter-Set4-Reverse-Hind III	CCC AAGCTT GCCTCTATTTGAAGGGTCTGG	
PDP1 Iso5-BamH1-Forward	CGC GGATCC GCCACC ATG CCA GCA CCAA CTCAAc	
PDP1-Not1-Reverse	ATTT GCGGCCGC CTATTCTTGGTTTTGATA	
PDP1-qPCR-Forward primer	TTCTGGAGCCACTGCTTGTGTG	qRT-PCR (mRNA)
PDP1-qPCR-Reverse primer	ACAGCGTGACTGCTGACCATGA	qRT-PCR (mRNA)
EGR1-ATG-HindIII-F	CCCAAGCTTATGGCCGCGGCCAAGGCCGA	EGR1-full length cDNA
EGR1-STOP-XhoI-R	CCGCTCGAGTTAGCAAATTTCAATTGTCC	EGR1-full length cDNA
shEGR1#8 duplex	AGCTAAAAAGAAGGTCTATTGGCCAACAATTCTCTTGAAATTGTTGGCCAATAGACCTTCGG GATCCCGAAGGTCTATTGGCCAACAATTTCAAGAGAATTGTTGGCCAATAGACCTTCTTTTT	shRNA
sgEGR1 #9 duplex	AGCTAAAAAGTGATGATGCTGTGACAATAATCTCTTGAATTATTGTCACAGCATCATCACGG GATCCCGTGATGATGCTGTGACAATAATTCAAGAGATTATTGTCACAGCATCATCACTTTTT	shRNA

Cell lines	**orignially from the American Type Culture Collection (ATCC), engineered and used by previous studies, authenticated by gene expression profiling**	
TMD8	Ngo, et al. Nature 2006	DOI: 10.1038/nature04687
OCI-Ly10	Ngo, et al. Nature 2006	DOI: 10.1038/nature04687
SUDHL2	Ngo, et al. Nature 2006	DOI: 10.1038/nature04687
OCI-Ly3	Ngo, et al. Nature 2006	DOI: 10.1038/nature04687
JEKO-1	Li, et al. Oncogene 2016	DOI: 10.1038/onc.2016.155
Granta519	Li, et al. Oncogene 2016	DOI: 10.1038/onc.2016.155
Rec-1	Li, et al. Oncogene 2016	DOI: 10.1038/onc.2016.155
Z138	Li, et al. Oncogene 2016	DOI: 10.1038/onc.2016.155
Rec-1	Li, et al. Oncogene 2016	DOI: 10.1038/onc.2016.155
Mino	Li, et al. Oncogene 2016	DOI: 10.1038/onc.2016.155

Supplemental References

1. Ngo VN, Davis RE, Lamy L, et al. A loss-of-function RNA interference screen for molecular targets in cancer. *Nature*. 2006;441(7089):106-110.
2. Ngo VN, Young RM, Schmitz R, et al. Oncogenically active MYD88 mutations in human lymphoma. *Nature*. 2011;470(7332):115-119.
3. Lu L, Zhu F, Zhang M, et al. Gene regulation and suppression of type I interferon signaling by STAT3 in diffuse large B cell lymphoma. *Proc Natl Acad Sci U S A*. 2018;115(3):E498-E505.
4. Chen S, Zhou Y, Chen Y, Gu J. fastp: an ultra-fast all-in-one FASTQ preprocessor. *Bioinformatics*. 2018;34(17):i884-i890.
5. Kim D, Paggi JM, Park C, Bennett C, Salzberg SL. Graph-based genome alignment and genotyping with HISAT2 and HISAT-genotype. *Nat Biotechnol*. 2019;37(8):907-915.
6. Zhang Y, Liu T, Meyer CA, et al. Model-based analysis of ChIP-Seq (MACS). *Genome Biol*. 2008;9(9):R137.
7. Kent WJ, Zweig AS, Barber G, Hinrichs AS, Karolchik D. BigWig and BigBed: enabling browsing of large distributed datasets. *Bioinformatics*. 2010;26(17):2204-2207.
8. Yu G, Wang LG, He QY. ChIPseeker: an R/Bioconductor package for ChIP peak annotation, comparison and visualization. *Bioinformatics*. 2015;31(14):2382-2383.
9. Zhu LJ, Gazin C, Lawson ND, et al. ChIPpeakAnno: a Bioconductor package to annotate ChIP-seq and ChIP-chip data. *BMC Bioinformatics*. 2010;11:237.
10. Bailey TL, Elkan C. Fitting a mixture model by expectation maximization to discover motifs in biopolymers. *Proc Int Conf Intell Syst Mol Biol*. 1994;2:28-36.
11. Gupta S, Stamatoyannopoulos JA, Bailey TL, Noble WS. Quantifying similarity between motifs. *Genome Biol*. 2007;8(2):R24.

Supplemental Figures and Figure Legends:

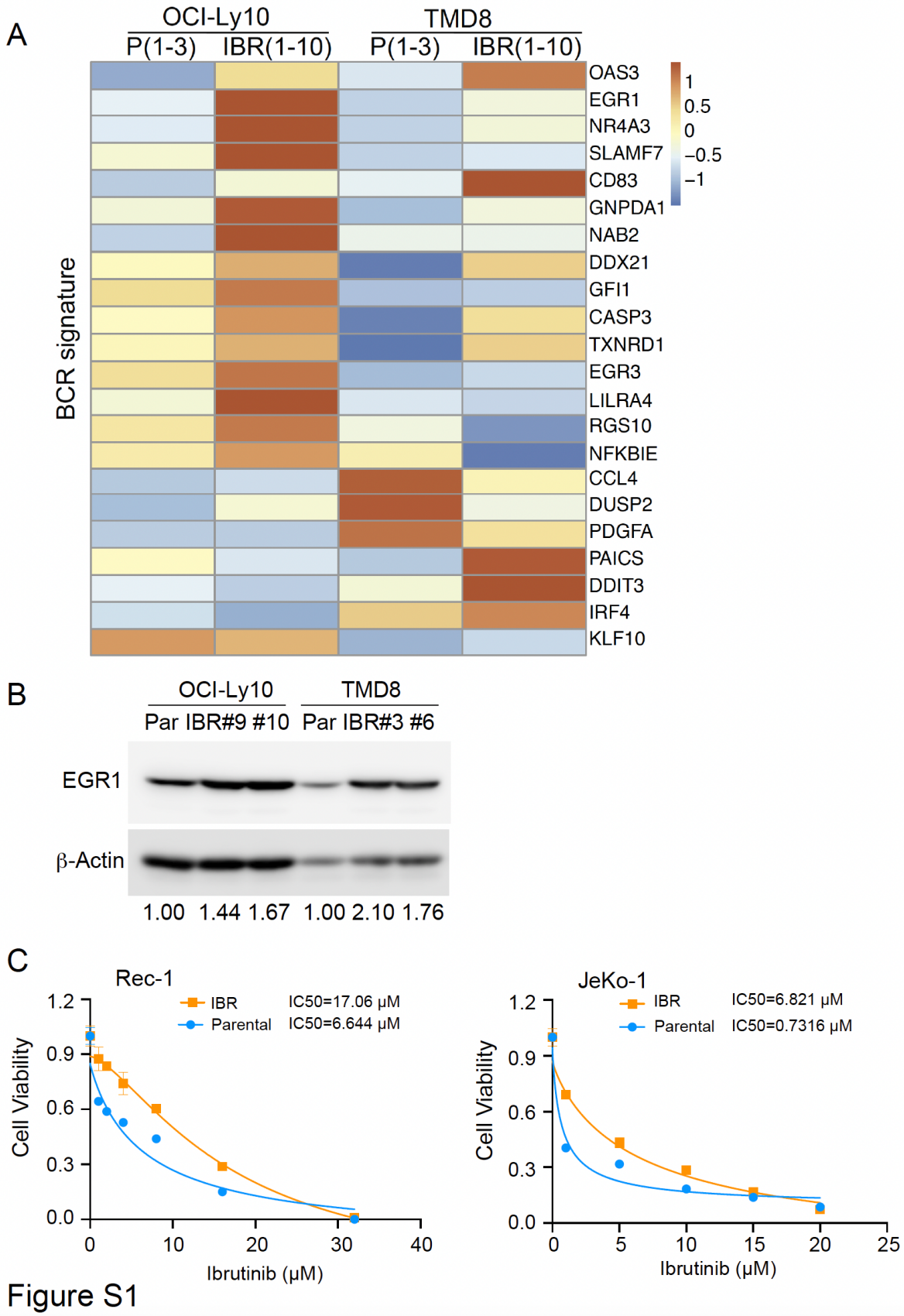

Figure S1

Supplemental Figure 1. Increased expression of BCR signaling pathway genes in ibrutinib-resistant cells. (A) Heat maps show differential expression of BCR signature genes between OCl-ly10 and TMD8 parental (P) (n=3) and IBR clones (n=10). (B) Immunoblot analysis of EGR1 expression in IBR clones versus parental cells in the ibrutinib-free culture for a month. β-Actin served as a loading control. (C) CellTiter-Glo™ Luminescent Cell Viability Assay after 3-day ibrutinib treatment in Rec-1 and JeKo-1 parental and IBR cells. IC50 was calculated by GraphPad Prism (9.0) using a 4-parameter nonlinear regression model.

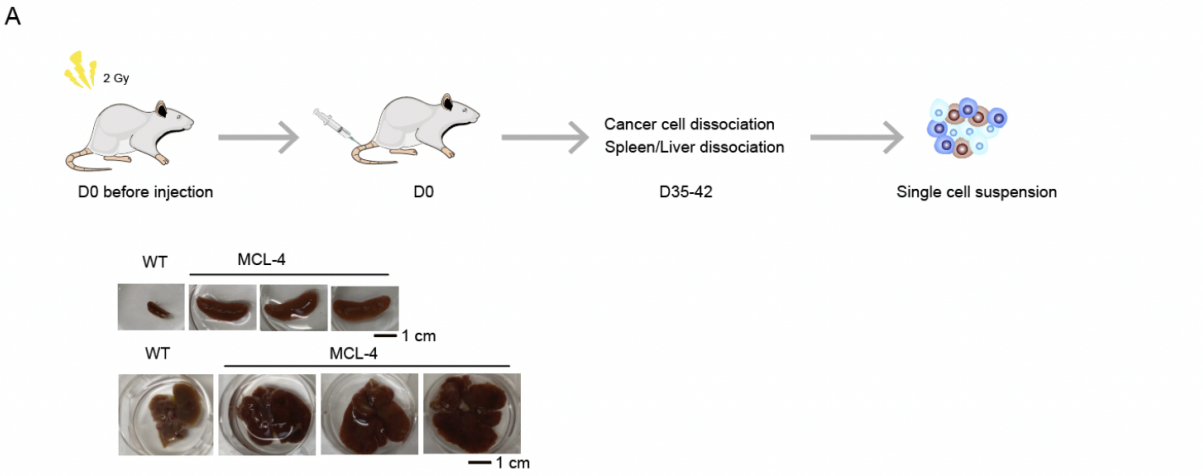
A
2 Gy
D0 before injection
D0
Cancer cell dissociation
Spleen/Liver dissociation
D35-42
Single cell suspension
WT
MCL-4
1 cm
WT
MCL-4
1 cm

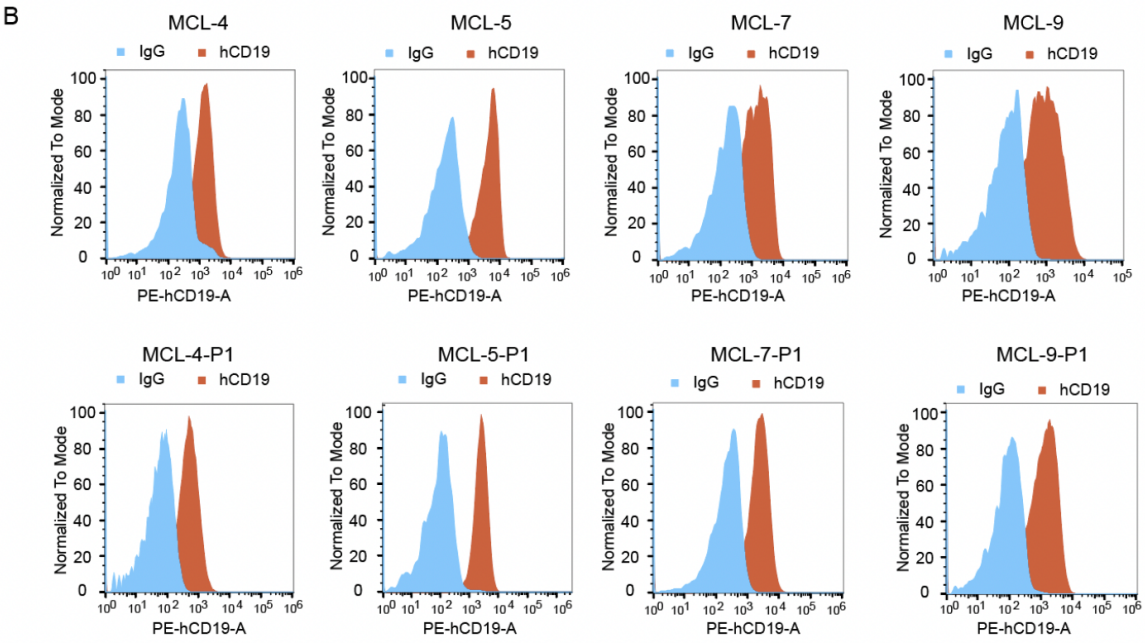
B
MCL-4
MCL-5
MCL-7
MCL-9
IgG
hCD19
Normalized To Mode
PE-hCD19-A
MCL-4-P1
MCL-5-P1
MCL-7-P1
MCL-9-P1

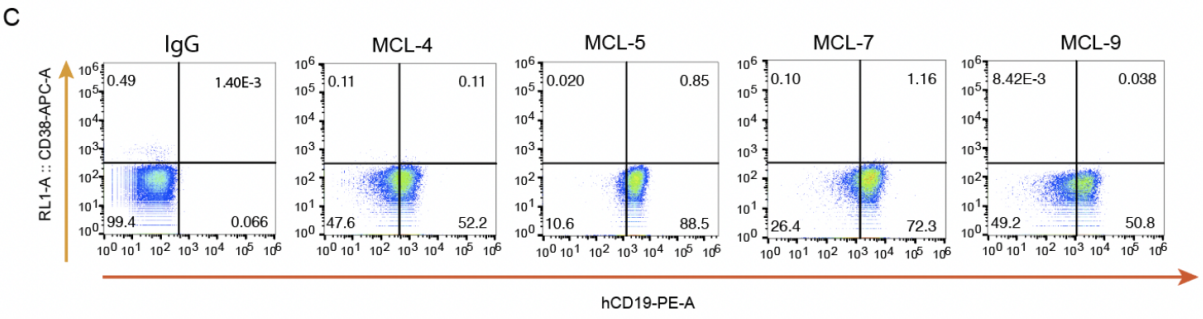
C
IgG
MCL-4
MCL-5
MCL-7
MCL-9
RL1-A :: CD38-APC-A
hCD19-PE-A
0.49
1.40E-3
99.4
0.066
0.11
0.11
47.6
52.2
0.020
0.85
10.6
88.5
0.10
1.16
26.4
72.3
8.42E-3
0.038
49.2
50.8

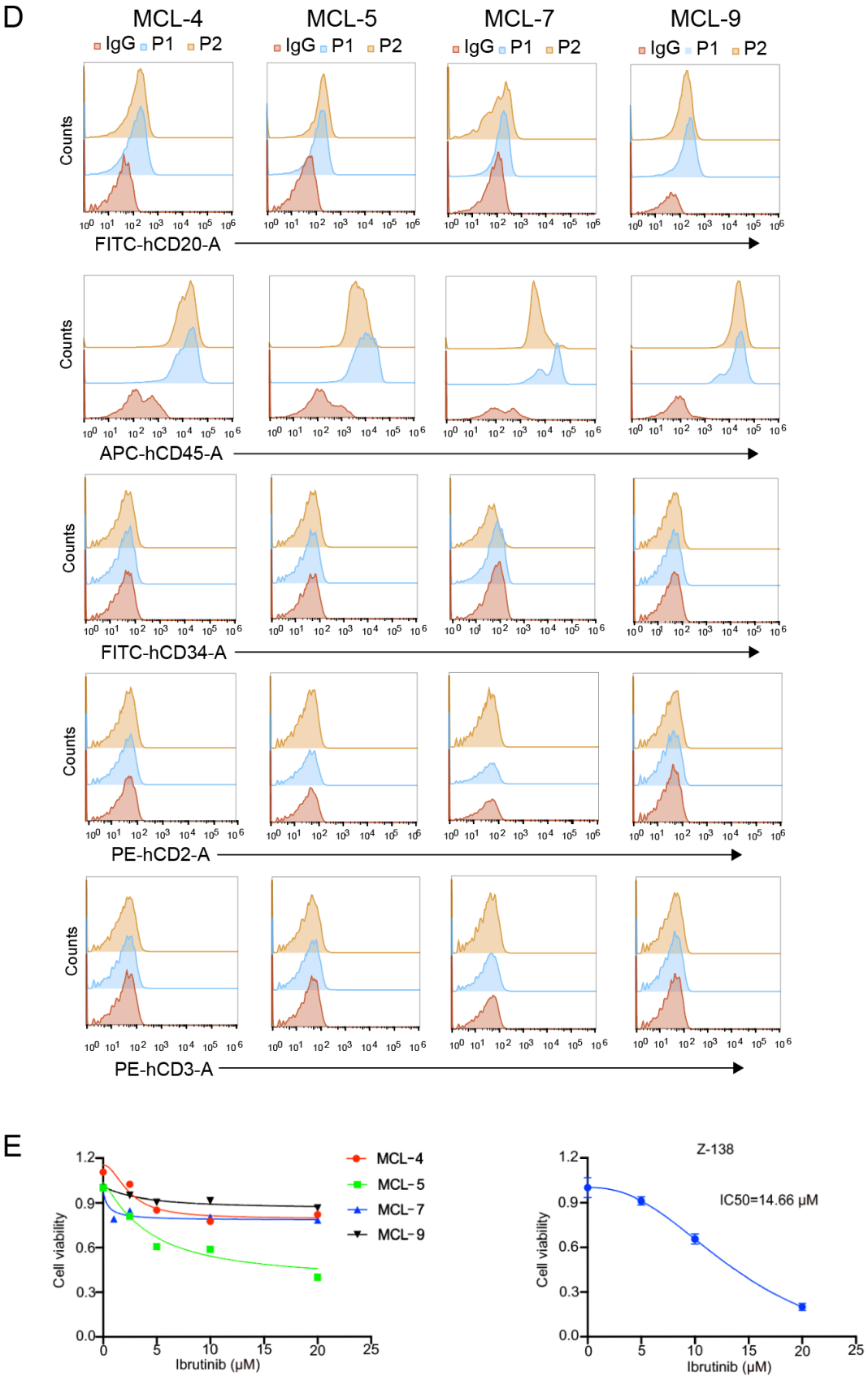
D
MCL-4
MCL-5
MCL-7
MCL-9
IgG P1 P2
Counts
FITC-hCD20-A
APC-hCD45-A
FITC-hCD34-A
PE-hCD2-A
PE-hCD3-A
E
MCL-4
MCL-5
MCL-7
MCL-9
Cell viability
Ibrutinib (μM)
Z-138
IC50=14.66 μM

Figure S2

Supplemental Figure 2. No phenotypical changes of primary MCL cells after expansion in NSG mice. (A) Schematic illustration of expansion of MCL patient derived cells in NSG mice (top). 2 x 10^6 MCL cells were resuspended in 0.1 ml PBS and injected into the tail-vein of sublethally irradiated (2 Gy) NSG mice. After 35-42 days, spleens and livers of mice were collected to obtain single-cell suspensions of tumor. Representative images of spleen and liver from wild type or PDX mice were shown (bottom). (B) Flow cytometry was used to determine human (h) CD19 expression in original (P0) MCL samples and MCL samples with one passage (P1) in NSG mice. (C) hD19 expression and hCD38 expression were determined by flow cytometry in four P1 MCL samples. (D) The expression of human CD20, human CD45, human CD34, human CD2 and human CD3 were determined by flow cytometry in four P1 MCL samples and MCL samples with two passages (P2) in NSG mice. (E) Trypan blue cell viability assay after 3-day ibrutinib treatment in MCL-4, MCL-5, MCL-7, MCL-9 cells (Left panel) and Z-138 (Right panel), P0 MCL samples were used in this assay. IC50 was calculated by GraphPad Prism (9.0) using a 4-parameter nonlinear regression model.

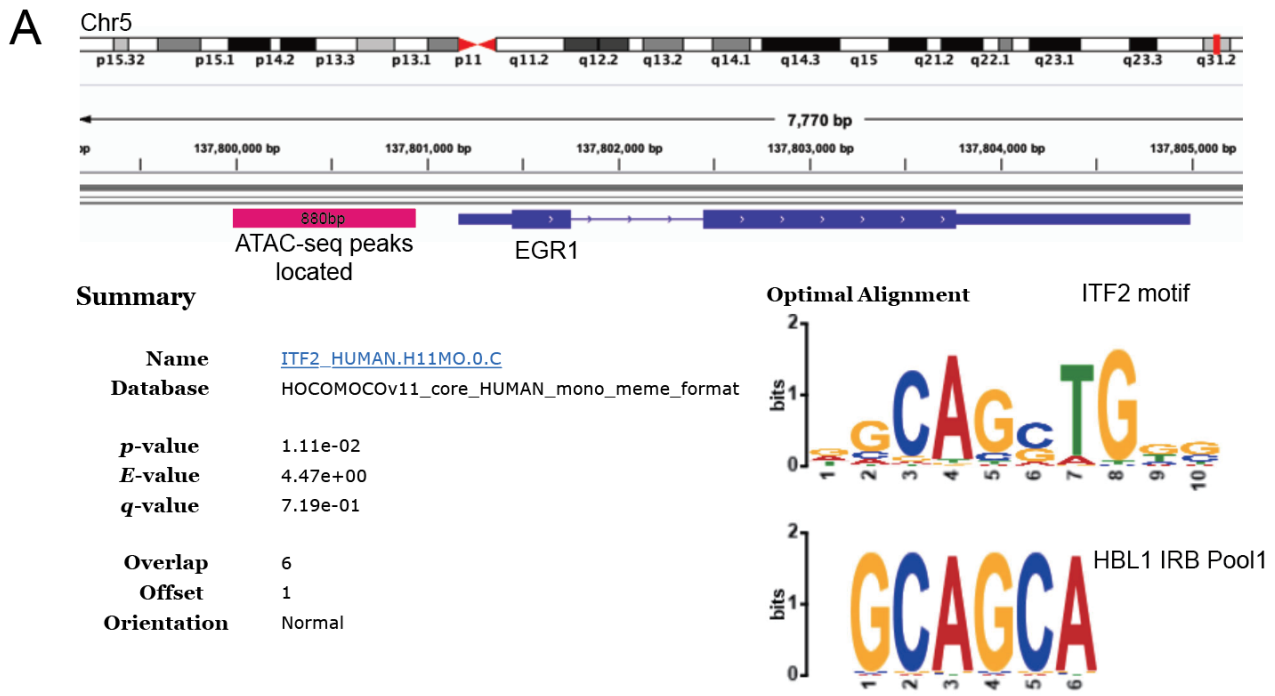

Figure S3

Supplemental Figure 3. Motif enrichment analysis of ATAC-seq in ibrutinib-resistant cells. (A) Motif enrichment analysis of ATAC-seq identified a high frequency of TCF4 motif (ITF2) on the EGR1 promoter region in ibrutinib-resistant cells.

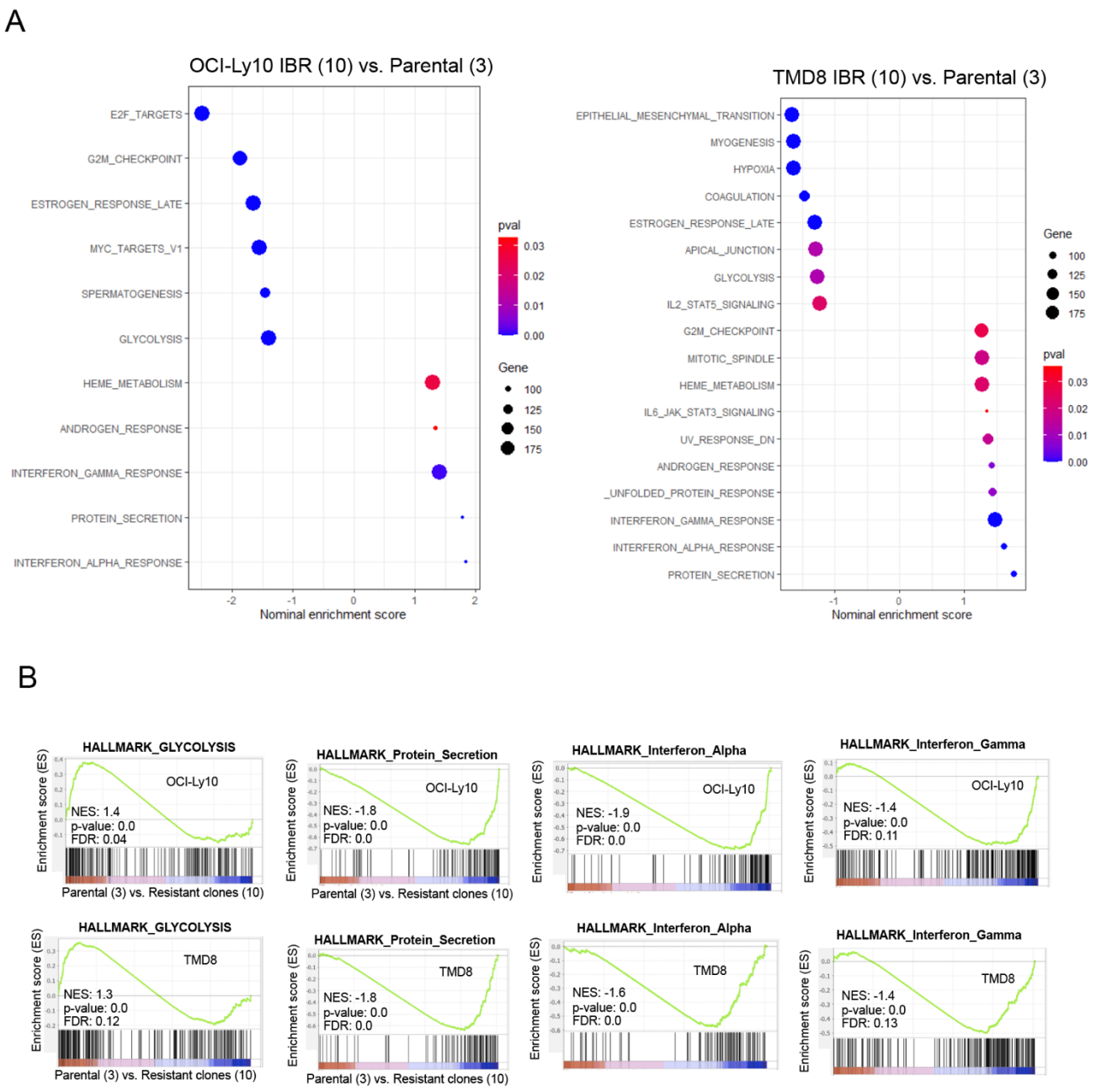

Figure S4

Supplemental Figure 4. Pathway enrichment analysis of RNA-seq data in ibrutinib-resistant cells. (A) A rank order list of the most enriched pathways in OCl-ly10 and TMD8 IBR clones (n=10) versus parental cells (P) (n=3). (B) Gene set enrichment analysis of glycolysis signature genes and protein secretion and interferon signaling signature genes in TMD8 and OCI-Ly10 parental and resistant cells. NES = normalized enrichment score. FDR = false discovery rate.

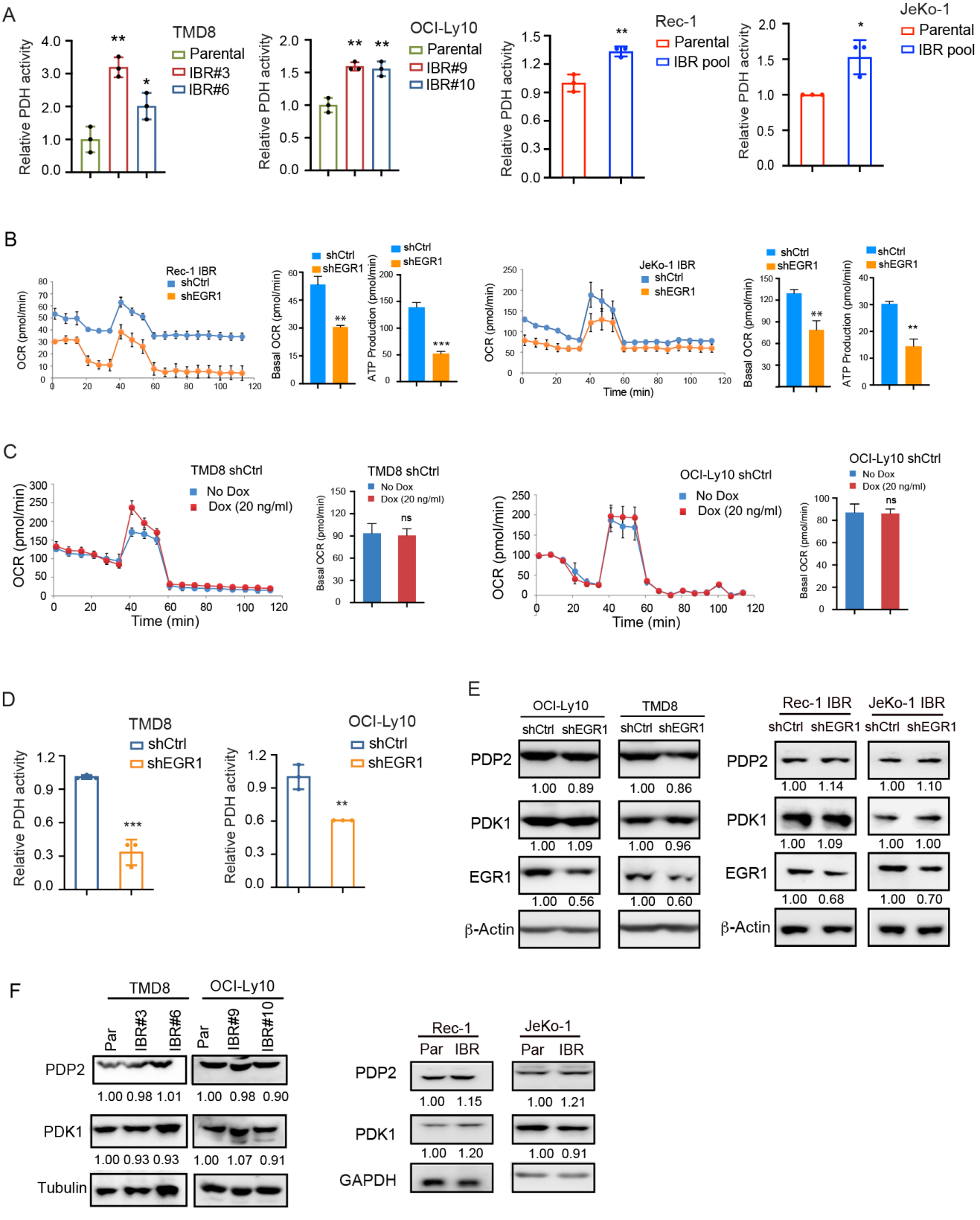
A
TMD8
Parental
IBR#3
IBR#6
OCI-Ly10
Parental
IBR#9
IBR#10
Rec-1
Parental
IBR pool
JeKo-1
Parental
IBR pool
Relative PDH activity
B
Rec-1 IBR
shCtrl
shEGR1
JeKo-1 IBR
OCR (pmol/min)
Time (min)
Basal OCR (pmol/min)
ATP Production (pmol/min)
C
TMD8 shCtrl
No Dox
Dox (20 ng/ml)
OCI-Ly10 shCtrl
ns
D
TMD8
OCI-Ly10
shCtrl
shEGR1
E
OCI-Ly10
TMD8
Rec-1 IBR
JeKo-1 IBR
PDP2
PDK1
EGR1
β-Actin
1.00 0.89
1.00 0.86
1.00 1.14
1.00 1.10
1.00 1.09
1.00 0.96
1.00 1.09
1.00 1.00
1.00 0.56
1.00 0.60
1.00 0.68
1.00 0.70
F
TMD8
OCI-Ly10
Par
IBR#3
IBR#6
IBR#9
IBR#10
PDP2
PDK1
Tubulin
1.00 0.98 1.01
1.00 0.98 0.90
1.00 0.93 0.93
1.00 1.07 0.91
Rec-1
JeKo-1
Par
IBR
GAPDH
1.00 1.15
1.00 1.21
1.00 1.20
1.00 0.91

Figure S5

Supplemental Figure 5. Analyses of PDH activity and OCR in ibrutinib-resistant cells or cells after EGR1 knockdown. (A) PDH activity assays in ABC DLBCL TMD8 and OCI-Ly10 parental cells and indicated clones, Rec-1 and JeKo-1 parental and resistant cells. Error bars represent mean ± SD of three replicates (**p<0.01, *p<0.05). (B) Reduced basal OCR and ATP production after EGR1 knockdown in ibrutinib-resistant MCL cells. Error bars represent mean ± SD of three replicates (**p<0.01, ***p<0.001). (C) OCR assay were performed in TMD8 and OCI-Ly10 control shRNA (shCtrl) cells with or without 20 ng/ml doxycycline treatment. Error bars represent mean ± SD of three replicates. (D) PDH activity assay after EGR1 knockdown in ABC DLBCL cells. Error bars represent mean ± SD of three replicates (**p<0.01, ***p<0.001). (E) Immunoblot analysis of PDP2 and PDK1 expression after EGR1 knockdown in ABC DLBCL and MCL cells. β-Actin served as a loading control. (F) Immunoblot analysis of PDP2 and PDK1 expression in IBR clones versus parental cells in ABC DLBCL cells, MCL parental and resistant cells. Tubulin and GAPDH served as a loading control.

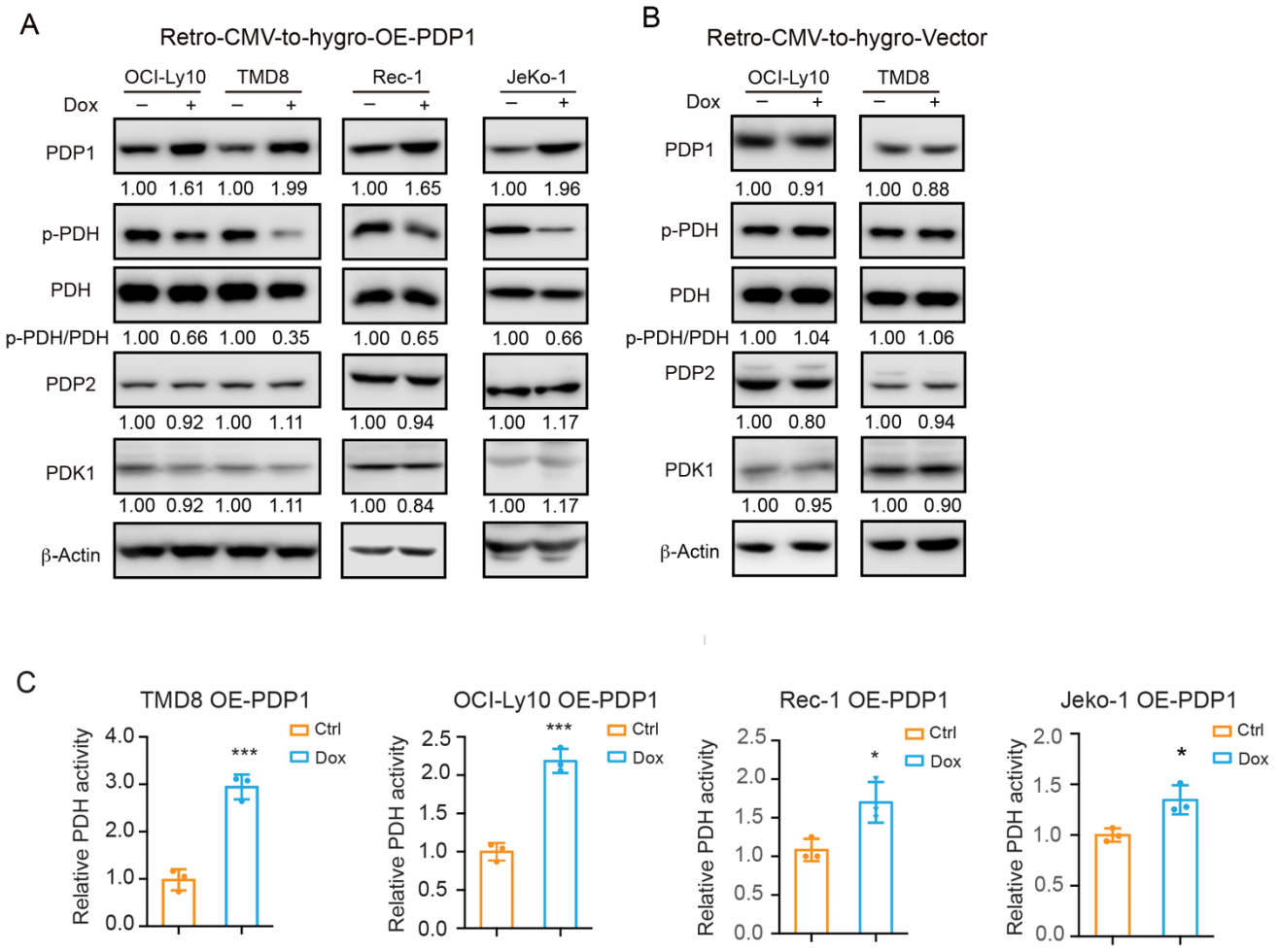

Figure S6

Supplemental Figure 6. PDP1 overexpression increases PDH activity in ABC DLBCL and MCL cells. (A) Immunoblot analysis of PDP1, p-PDH, PDH, PDP2 and PDK1 expression after retrovirally inducible PDP1 expression in ABC DLBCL and MCL cells treated with 20 ng/ml doxycycline for 3 days. β-Actin served as a loading control. (B) Immunoblot analysis of PDP1, p-PDH, PDH, PDP2 and PDK1 expression after retrovirally inducible empty vector in ABC DLBCL cells. β-Actin served as a loading control. (C) PDH activity assay after retrovirally inducible PDP1 expression in ABC DLBCL and MCL cells treated with 20 ng/ml doxycycline for 3 days. Error bars represent mean ± SD of three replicates (*p<0.05, ***p<0.001).

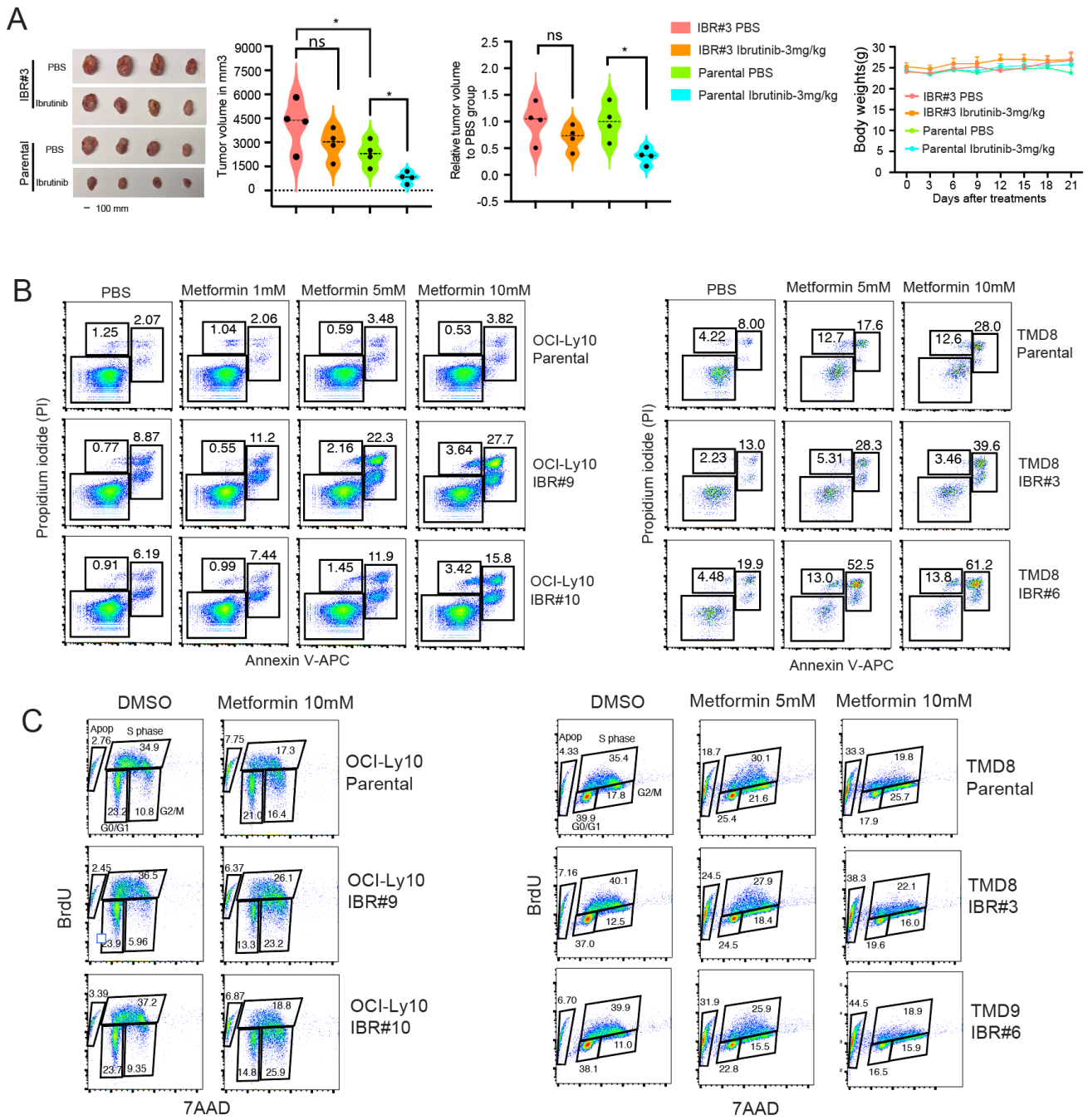
A
IBR#3
PBS
Ibrutinib
Parental
PBS
Ibrutinib
100 mm
Tumor volume in mm3
ns
*
*
Relative tumor volume to PBS group
ns
*
IBR#3 PBS
IBR#3 Ibrutinib-3mg/kg
Parental PBS
Parental Ibrutinib-3mg/kg
Body weights(g)
Days after treatments
B
PBS
Metformin 1mM
Metformin 5mM
Metformin 10mM
OCI-Ly10 Parental
OCI-Ly10 IBR#9
OCI-Ly10 IBR#10
Propidium iodide (PI)
Annexin V-APC
TMD8 Parental
TMD8 IBR#3
TMD8 IBR#6
C
DMSO
Metformin 10mM
Metformin 5mM
OCI-Ly10 Parental
OCI-Ly10 IBR#9
OCI-Ly10 IBR#10
TMD8 Parental
TMD8 IBR#3
TMD9 IBR#6
BrdU
7AAD
Apop
S phase
G0/G1
G2/M
D
SUDHL2
OCI-Ly3
Ibrutinib (nM) Alone
Metformin (mM) Alone
Ib (10nM) + Met (mM)
Cell viability relative to DMSO
Ibrutinib (nM)
Metformin (nM)

Figure S7

Supplemental Figure 7. Xenograft analysis of ibrutinib-resistant cells and their parental cells upon ibrutinib treatment, and cell cycle and apoptosis analyses in ibrutinib-resistant cells and their parental cells upon metformin treatment. (A) TMD8 parental and ibrutinib-resistant xenografts. TMD8 parental and ibrutinib-resistant cells were established as a subcutaneous tumor (average 150 mm^3) in NSG mice, and then treated with 3 mg/kg ibrutinib (i.p.) daily until the endpoint (day 21). Tumor images and tumor volume of all four groups at the endpoint in the left two panels, relative tumor volume of ibrutinib treatments versus control groups in TMD8 ibrutinib resistant and parental cells in the middle panel, body weight changes during the treatment in each group in the right panel. Data are represented as mean ± SEM. Error bars represent mean ± SEM (One-way ANOVA, *$p<0.05$). (B) Flow cytometric analysis of cell apoptosis by Annexin V and propidium iodide (PI) staining in OCI-Ly10 and TMD8 parental and resistant cells after 3-day treatment with the indicated concentrations of metformin. (C) Cell cycle analysis by flow cytometry after 4 hours of BrdU incorporation in TMD8 and OCI-Ly10 parental and resistant cells after 3-day treatment with the indicated concentrations of metformin. (D) CellTiter-Glo™ Luminescent Cell Viability Assay of primary ibrutinib-resistant SUDHL2 or OCI-Ly3 cells after 3 days of treatment with ibrutinib, metformin or a combination of the two drugs. Error bars represent mean ± SD (One-way ANOVA, ***$p<0.001$, n=3).

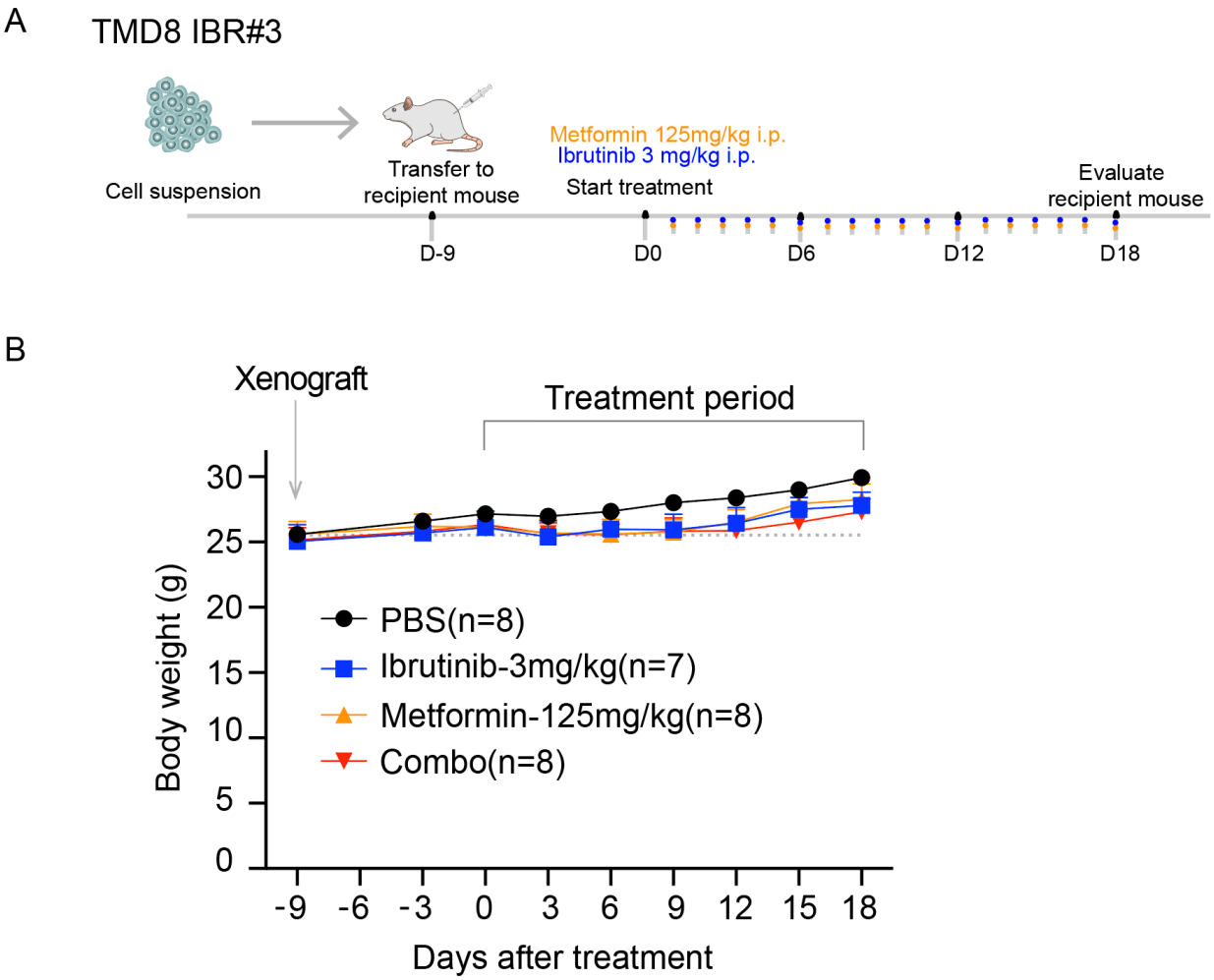

Figure S8

Supplemental Figure 8. Schematic illustration of ibrutinib-resistant ABC DLBCL xenografts.
(A) Schematic illustration of ibrutinib-resistant ABC DLBCL xenografts and the treatment procedure. (B) Body weight changes during the treatment in each group. Data are represented as mean ± SEM.

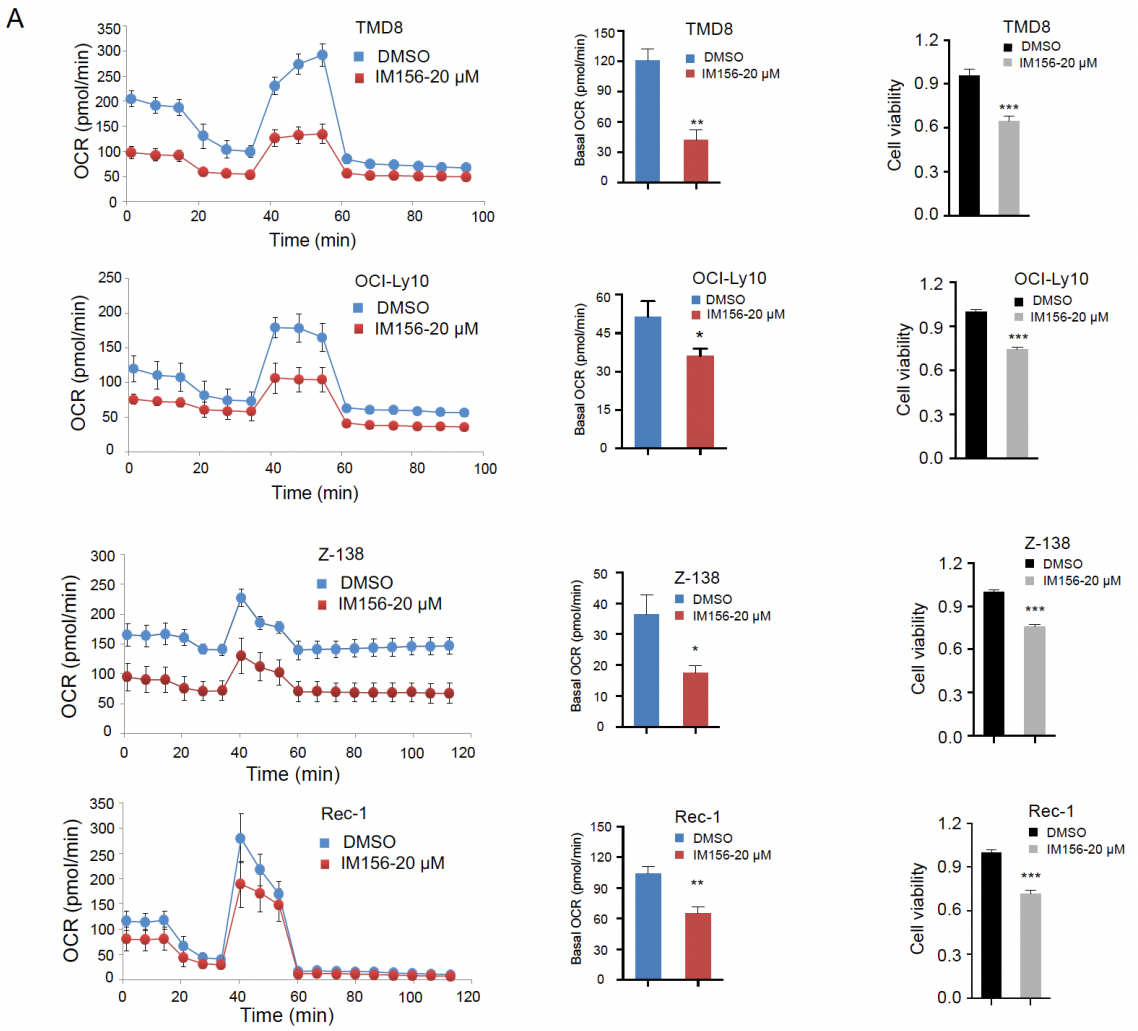

B Synergy scores

Samples	Drug Combination	Synergy score	Most synergistic area score	Method
SUDHL-2	Ibru-IM156	21.309	31.924	HSA
OCI-Ly10 IBR#10	Ibru-IM156	19.302	22.643	HSA
OCI-Ly10	Ibru-IM156	10.17	11.733	HSA
TMD8	Ibru-IM156	25.972	33.891	HSA

Synergy scores

Samples	Drug Combination	Synergy score	Most synergistic area score	Method
MCL-4	Ibru-IM156	19.807	22.287	HSA
MCL-5	Ibru-IM156	24.885	30.158	HSA
MCL-7	Ibru-IM156	16.114	19.669	HSA
MCL-9	Ibru-IM156	8.246	11.473	HSA

Synergy scores

Samples	Drug Combination	Synergy score	Most synergistic area score	Method
Granta-519	Ibru-IM156	16.513	33.131	HSA
Z-138	Ibru-IM156	8.079	14.229	HSA
Mino	Ibru-IM156	11.047	15.82	HSA
Rec-1	Ibru-IM156	18.852	32.454	HSA
JeKo	Ibru-IM156	14.319	22.518	HSA

Figure S9

Supplemental Figure 9. OCR analysis after IM156 treatment and synergy scores in ABC DLBCL and MCL cell lines and primary MCL cells after IM156 and ibrutinib treatment. (A) OCRs were

determined by Seahorse XFe96 extracellular flux analyzer (Left panel). Reduced basal OCR after 3-days treatment with IM156 (20 μM) in ABC DLBCL and MCL cells (Middle panel). Cell viability was determined by trypan blue staining after 3-day treatment with IM156 (20 μM) (Right panel). Error bars represent mean ± SD (*p<0.05,**p<0.01. ***p<0.001, n=3). (B) Synergy scores were calculated by online SynergyFinder 2.0 (https://synergyfinder.fimm.fi/synergy/20201021224844908442/) based on the HSA model. A score above 0 indicated a synergistic effect of the two drugs.